THE JOURNAL OF BIOLOGICAL CHEMISTRY VOL. 286, NO. 46, pp. 40401–40412, November 18, 2011

Regulation of RCAN1 Protein Activity by Dyrk1A Protein-mediated Phosphorylation*[S]

Received for publication, April 22, 2011, and in revised form, September 21, 2011 Published, JBC Papers in Press, September 30, 2011, DOI 10.1074/jbc.M111.253971

Min-Su Jung, Jung-Hwa Park, Young Shin Ryu, Sun-Hee Choi, Song-Hee Yoon, Mi-Yang Kwen, Ji Youn Oh, Woo-Joo Song[1], and Sul-Hee Chung[2]

From the Graduate Program in Neuroscience, Institute for Brain Science and Technology, FIRST Research Group, Inje University, 633-146 Gaegeum-2-Dong, Busanjin-Gu, Busan 614-735, South Korea

Two genes on chromosome 21, namely dual specificity tyrosine phosphorylation-regulated kinase 1A (*Dyrk1A*) and regulator of calcineurin 1 (*RCAN1*), have been implicated in some of the phenotypic characteristics of Down syndrome, including the early onset of Alzheimer disease. Although a link between Dyrk1A and RCAN1 and the nuclear factor of activated T cells (NFAT) pathway has been reported, it remains unclear whether Dyrk1A directly interacts with RCAN1. In the present study, Dyrk1A is shown to directly interact with and phosphorylate RCAN1 at Ser^{112} and Thr^{192} residues. Dyrk1A-mediated phosphorylation of RCAN1 at Ser^{112} primes the protein for the GSK3β-mediated phosphorylation of Ser^{108}. Phosphorylation of RCAN1 at Thr^{192} by Dyrk1A enhances the ability of RCAN1 to inhibit the phosphatase activity of calcineurin (Caln), leading to reduced NFAT transcriptional activity and enhanced Tau phosphorylation. These effects are mediated by the enhanced binding of RCAN1 to Caln and its extended half-life caused by Dyrk1A-mediated phosphorylation. Furthermore, an increased expression of phospho-Thr^{192}-RCAN1 was observed in the brains of transgenic mice overexpressing the Dyrk1A protein. These results suggest a direct link between Dyrk1A and RCAN1 in the Caln-NFAT signaling and Tau hyperphosphorylation pathways, supporting the notion that the synergistic interaction between the chromosome 21 genes *RCAN1* and *Dyrk1A* is associated with a variety of pathological features associated with DS.

Down syndrome (DS[3]; also known as Trisomy 21) is a very common genetic disorder caused by the presence of an extra copy of human chromosome 21. The genes that encode dual specificity tyrosine phosphorylation-regulated kinase 1A (*Dyrk1A*) and regulator of calcineurin 1 (*RCAN1*) are both located on chromosome 21 and might be responsible for certain clinical features of DS, such as mental retardation and early onset Alzheimer disease (AD). Dyrk1A is a dual specificity protein kinase that is activated by autophosphorylation on a tyrosine residue in the activation loop, and it phosphorylates serine or threonine residues in substrate proteins (1). Dyrk1A is a multifunctional protein kinase with various substrates, such as transcription factors, splicing factors, and synapse-associated proteins (2, 3). Dyrk1A contains a nuclear localization sequence at its N terminus and locates both to the cytosol and nucleus, phosphorylating nuclear and cytoplasmic substrate proteins. Dyrk1A also functions as a priming kinase for GSK3β phosphorylation of proteins such as Tau and NFAT (4, 5). The protein encoded by *Dyrk1A* is considered a candidate protein potentially responsible for DS mental retardation (6–9) and early onset of AD-like symptoms (3, 10–14) in DS patients. Transgenic mice overexpressing Dyrk1A (Dyrk1A TG mice) show severe hippocampus-dependent learning and memory defects (15–17). We recently reported that overexpression of Dyrk1A in DS brains may contribute to early onset of AD through hyperphosphorylation of Tau and enhancement of Aβ production, potentially due to the phosphorylation of APP and presenilin 1 (10, 11, 14). Dyrk1A also plays a critical role in neurodevelopment, including neuronal differentiation and synaptic plasticity (18).

RCAN1, formerly known as Down syndrome critical region 1 (DSCR1), acts as an endogenous regulator of calcineurin (Caln), a ubiquitous and multifunctional calcium-activated serine/threonine protein phosphatase. Its overexpression either in animal models or in cells results in the inhibition of signaling pathways that are controlled by the nuclear factor of activated T cells (NFAT) transcription factor (19). RCAN1 is widely expressed in the brain (20), both during development and in adults. RCAN1$^{-/-}$ mice show impairments in spatial learning and memory (21), and knockdown or overexpression of the *Drosophila melanogaster* RCAN1 homolog leads to severe learning defects (22). RCAN1 has therefore been proposed as a candidate protein responsible for mental retardation in DS. RCAN1 has also been implicated in oxidative stress and exocytosis (23, 24).

Increased expression of certain genes on chromosome 21, alone or in cooperation, is thought to be responsible for the DS phenotype, including mental retardation, congenital heart defects, gastrointestinal malformations, immune and endocrine system defects, and early onset of dementia of the

* This work was supported by a grant from the Korea Healthcare Technology R&D Project and Ministry of Health, Welfare, and Family Affairs, Republic of Korea, Grants A092004 and A080227. This work was also supported by the Basic Science Research Program through the National Research Foundation of Korea funded by the Ministry of Education, Science, and Technology (Grants 2009-0073210, 2009-0067388, 2011-0014085, and 2011-0023401).

[S] The on-line version of this article (available at http://www.jbc.org) contains supplemental Figs. S1–S6.

[1] To whom correspondence may be addressed. Tel.: 82-51-892-4186; Fax: 82-51-892-0059; E-mail: wjsong@inje.ac.kr.

[2] To whom correspondence may be addressed. Tel.: 82-51-892-4185; Fax: 82-51-892-0059; E-mail: sulchung@inje.ac.kr.

[3] The abbreviations used are: DS, Down syndrome; AD, Alzheimer disease; Caln, calcineurin; NFAT, nuclear factor of activated T cells; RIPA, radioimmune precipitation assay; CaM, calmodulin; TG, transgenic; p-Tau212, phospho-Thr^{212}-Tau; p-Tau404, phospho-Ser^{404}-Tau; pT192-RCAN1, phospho-Thr^{192}-RCAN1.

Alzheimer type. Increased expression of RCAN1 and Dyrk1A in individuals with DS destabilizes the NFAT genetic circuit (25). Increased Dyrk1A or RCAN1 expression has been reported in both human DS and AD brains (12, 26–29). The present study investigated the possible direct link between Dyrk1A and RCAN1 and examined the effect of Dyrk1A-mediated phosphorylation on RCAN1 activity in relation to the pathological traits of DS.

EXPERIMENTAL PROCEDURES

Proteins and Antibodies—Mouse wild-type and Y321F kinase-inactive mutant Dyrk1A proteins with endogenous 13-histidine repeats were purified with Ni^{2+}-NTA resin as described previously (10). Full-length human RCAN1-1S (RCAN1) and human Caln A cDNAs were cloned into pET29b and pET28b, respectively. The full-length human RCAN1 and an RCAN1 C-terminal (RCAN1Ct) cDNA corresponding to exon 7 were cloned into pGEX4T-3. The recombinant proteins were expressed in *Escherichia coli* BL21(DE3) strain RIL (Stratagene) and purified using Ni^{2+}-NTA or glutathione-Sepharose 4B resin.

Anti-α-tubulin and HA antibodies were from Sigma. The anti-Caln antibody was from R&D Systems. The anti-Dyrk1A antibody was custom-made as described previously (16). The anti-RCAN1 antibodies were either from Abnova or custom-made using synthetic peptides, RPEYTPIHLS. A phosphospecific RCAN1 antibody to a synthetic phosphopeptide (^{188}RPEYpTPIHLS^{197}) was generated and affinity-purified first with a cognate nonphosphopeptide (RPEYTPIHLS) affinity column and then with a phosphopeptide column (Peptron, Inc., Daejeon, South Korea).

Plasmids, siRNAs, and Cell Transfection—The full-length wild-type and Y321F kinase-inactive Dyrk1A mutant cDNAs were cloned into pcDNA3.1 as described previously (10). The full-length human wild-type RCAN1-1S (RCAN1) and Caln A cDNAs were cloned into pcDNA3.1 (Invitrogen). Phosphorylation-defective mutants of RCAN1 cDNA were generated by DpnI-mediated site-directed mutagenesis (Stratagene), and the clones were verified by sequencing. For the siRNA experiment, the *Dyrk1A*-specific siRNA (5′-AUGGAGCUAUGGACGUUAA) with the TT overhang was designed and synthesized by Samchully Pharm Co. Ltd. (Seoul, South Korea). For siRNA delivery, Dyrk1A-specific duplex siRNA (100 pmol for a 6-well plate) was transfected into PC12 cells (7.5×10^5 cells/well) using Lipofectamine 2000 (Invitrogen). *Dyrk1A* siRNA (5′-GUACAUCGUCAAGCUCAGGU) was used as an ineffective siRNA control. After 48–72 h of siRNA treatment, cell lysates were prepared for immunoblot analyses. HEK293T cells were transfected with the indicated plasmids using the calcium phosphate precipitation method. One day later, the cells were lysed in RIPA buffer (50 mM Tris, pH 8.0, 150 mM NaCl, 1% Nonidet P-40, 0.1% SDS, 0.5% deoxycholic acid) containing 1 mM PMSF, a phosphatase inhibitor mixture, and a protease inhibitor mixture (Calbiochem) and subjected to Western blot analysis.

Dyrk1A in Vitro Kinase Assay—For analysis by autoradiography, purified RCAN1 wild-type (WT) or mutant protein (100 ng) was incubated with recombinant full-length Dyrk1A protein (1 μg) for 1 h at 37 °C in kinase buffer (20 mM MOPS, pH 7.0, 10 mM $MgCl_2$, 1 mM DTT, and 20 μM sodium orthovanadate) containing 25 μM cold ATP and 5 μCi of [γ-^{32}P]ATP. The reaction mixtures were separated on SDS-polyacrylamide gels, and radioactive bands were detected with the Typhoon 9200 imaging system (Amersham Biosciences). The ability of Dyrk1A to prime RCAN1 WT or mutant proteins for GSK3β phosphorylation was examined by prephosphorylating GST fusion proteins bound to glutathione-Sepharose beads with 720 ng of Dyrk1A in the presence and absence of 1 mM non-radioactive ATP overnight at 30°C. After the non-radioactive priming step, the bead-bound GST fusion proteins were washed extensively to remove recombinant kinase and ATP. Phosphorylated GST fusion proteins were then incubated with 20 ng of GSK3β (Millipore) in a 25-μl final volume of the kinase buffer in the presence of 25 μM ATP and 10 μCi of [γ-^{32}P]ATP for 40 min at 37 °C and analyzed as described above.

Preparation of Lysates from Cell Cultures and Brains and Western Blot Analysis—HEK293T cells were harvested 24 h after transient transfection with the indicated plasmids. Cells were lysed in RIPA buffer with 1 mM PMSF and a protease inhibitor mixture. Transgenic mice overexpressing the human *Dyrk1A* gene, which was carried on a bacterial artificial chromosome, were generated and maintained as described previously (16). Experiments were performed in accordance with guidelines set forth by the Inje University Council directive for the proper care and use of laboratory animals. Mice were sacrificed by cervical dislocation. Brains were dissected, snap-frozen in liquid nitrogen, and Dounce-homogenized in RIPA buffer containing 1 mM PMSF, a protease inhibitor mixture, and 0.5 mM sodium orthovanadate. Protein concentration was determined using the BCA method (Sigma). Typically, 25–50 μg of the brain lysates was used for Western blotting. Densitometric quantification was carried out using ImageJ 1.42 software (National Institutes of Health, Bethesda, MD).

Co-immunoprecipitation and GST Pull-down Assay—For co-immunoprecipitation, brain lysates (2–6 mg) from the Dyrk1A TG mice or HEK293T cell lysates (500 μg) transfected with the indicated plasmids were incubated with control IgG (R&D Systems), anti-RCAN1, or anti-Dyrk1A antibodies overnight at 4 °C in RIPA buffer with protease inhibitors and 1 mM PMSF. The next day, after 1 h of incubation with protein A beads (Pierce), the bead mixture was gently washed with 1% Triton X-100 in RIPA buffer, and the bound proteins were subjected to immunoblot analysis with the indicated antibodies. For the GST pull-down assay, purified GST-RCAN1 WT or the phosphorylation-defective mutants were incubated with recombinant Dyrk1A protein (1 μg) or HEK293T cell lysates (500 μg) transfected with the plasmid encoding Caln for 1 h at 4 °C in binding buffer (50 mM Tris, pH 8.0, 100 mM NaCl, 10% glycerol, 2 mM β-mercaptoethanol, 0.01% Nonidet P-40, 0.5 mM EDTA, 1 mM PMSF). The beads were then washed with 300 mM NaCl-containing binding buffer three times, and the bound proteins were subjected to immunoblot analysis with the indicated antibodies.

Immunocytochemistry—PC12 cells were plated onto polyethyleneimine-coated coverslips, treated with nerve growth factor (NGF) for 6 days, and then fixed with 4% formaldehyde in

phosphate-buffered saline (PBS). For primary embryonic rat cortical cultures, embryonic day 17 pregnant Sprague-Dawley rats were purchased from Orient Bio Inc. (Seongnam-si, South Korea). The cortices of the embryos were dissected and cultured as described previously (30, 31). Primary cortical cultures were plated onto poly-D-lysine-coated glass coverslips and grown in neurobasal growth medium for 5 days before fixing with 4% formaldehyde in PBS. The fixed cells were subsequently permeabilized with 0.1% Triton X-100 and blocked with 5% bovine serum albumin (BSA) and then incubated for 2 h at room temperature with primary antibodies (rabbit anti-Dyrk1A antibody (1:50), mouse anti-RCAN1 antibody (1:50), or rabbit phosphospecific RCAN1 antibody (1:2,000)). The cells were then incubated with secondary antibodies (Texas Red-conjugated goat anti-rabbit or Alexa Fluor 488-conjugated goat anti-mouse antibodies at a 1:500 dilution) for 1 h at room temperature, washed with PBS, and examined using a fluorescence microscope (Olympus BX61) or a confocal laser scan microscope (LSM 510 META, Carl Zeiss).

Measurement of Caln Phosphatase Activity—The activity of Caln was determined using *p*-nitrophenyl phosphate as described previously (32). Phosphatase assays using 60 mM *p*-nitrophenyl phosphate (Sigma) were performed using 10 μg of purified recombinant Caln with and without purified recombinant RCAN1 WT or the phosphorylation-defective mutants (0.8 or 1.6 μg) and 200 nM calmodulin (CaM; Calbiochem) in assay buffer (100 mM Tris, pH 7.5, 100 mM NaCl, 0.5 mM DTT, 100 μg/ml BSA, 1 mM $MnCl_2$, 0.4 mM $CaCl_2$). In each assay, blank tubes containing buffer only were prepared to determine background levels of hydrolyzed *p*-nitrophenyl phosphate. Control tubes contained buffer and Caln/CaM. After 5 min of incubation at 30 °C, the reactions were initiated by the addition of 60 mM *p*-nitrophenyl phosphate. The tubes were incubated for an additional 60–90 min at 30 °C, and the liberation of *p*-nitrophenol was measured at 405 nm using a TECAN Infinite 200 plate reader.

NFAT-Luciferase Assay—For luciferase experiments, HEK293T cells grown in 24-well plates were transfected with 0.5 ng of pCMV-RL reporter (*Renilla* luciferase, internal standard), 200 ng of pGL3-Basic reporter (NFAT-luciferase, AP-1 promoter), and 50 ng of expression plasmids encoding empty vector, RCAN1 WT, or the phosphorylation-defective mutants. The total amount of plasmid was kept constant for all groups. After transfection, cells were treated with ionomycin (2.5 μM) for 48 h and analyzed for reporter gene activity using the Dual-Luciferase reporter assay (Promega) as recommended by the manufacturer. NFAT luciferase values were normalized to *Renilla* luciferase values.

RESULTS

Dyrk1A Interacts with RCAN1—To determine whether RCAN1 interacts with Dyrk1A, co-immunoprecipitation assays were carried out in HEK293T cells transfected with expression vectors encoding RCAN1 and Dyrk1A. RCAN1 co-immunoprecipitated with Dyrk1A, indicating that Dyrk1A interacts with RCAN1 (Fig. 1*A*). Furthermore, reverse co-immunoprecipitation experiments with the anti-RCAN1 antibody also revealed an interaction between Dyrk1A and RCAN1,

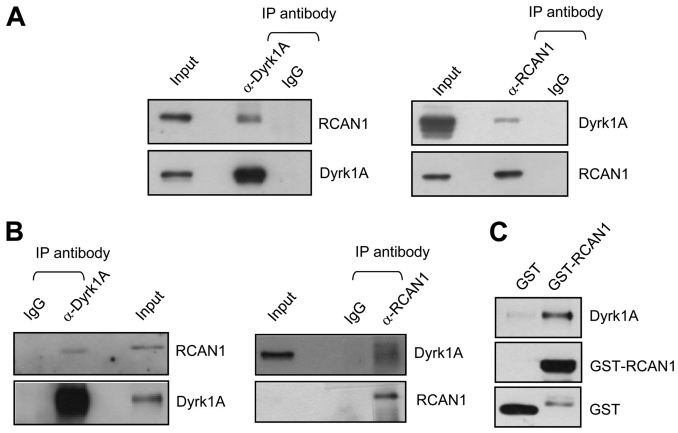

FIGURE 1. **RCAN1 interacts with Dyrk1A.** *A*, co-immunoprecipitation (*IP*) assay. HEK293T cell lysates transfected with plasmids encoding RCAN1 and Dyrk1A were immunoprecipitated with control IgG, anti-Dyrk1A (*left*), or anti-RCAN1 antibodies (*right*) and subjected to immunoblot analysis with the indicated antibodies. *B*, co-immunoprecipitation. Brain lysates (2–6 mg) from Dyrk1A TG mice were immunoprecipitated with control IgG or an anti-Dyrk1A antibody (*left*) or an anti-RCAN1 antibody (*right*) and subjected to immunoblot analysis with the indicated antibodies. *C*, GST pull-down assay to determine the direct interaction between Dyrk1A and RCAN1. Purified GST or a GST-RCAN1 fusion protein immobilized on beads was incubated with recombinant Dyrk1A protein and subjected to immunoblot analyses for Dyrk1A and GST.

as shown in Fig. 1*A*. To further determine whether endogenous RCAN1 and Dyrk1A interact in mammalian neurons, the brain lysates of Dyrk1A TG mice were immunoprecipitated with the anti-Dyrk1A or RCAN1 antibodies. RCAN1 associates with Dyrk1A in brain lysates (Fig. 1*B*). The direct interaction between purified Dyrk1A protein and GST-RCAN1 was further examined using a GST pull-down assay, which showed that GST-RCAN1 but not GST alone was able to bind directly to Dyrk1A as shown in Fig. 1*C*.

Dyrk1A Phosphorylates RCAN1 on Ser^{112} and Thr^{192} Residues—To determine whether Dyrk1A can phosphorylate RCAN1 *in vitro*, purified RCAN1 was incubated with recombinant Dyrk1A WT or inactive Dyrk1A Y321F mutant in a kinase assay buffer containing [γ-^{32}P]ATP. A band that migrated to a position corresponding to the molecular size of RCAN1 was detected by autoradiography only when both Dyrk1A WT and RCAN1 were present in the reaction mixture (Fig. 2*A*), indicating that RCAN1 was phosphorylated by active Dyrk1A. *In vitro* kinase assays in the presence of [γ-^{32}P]ATP were also performed with the RCAN1-Dyrk1A immunocomplexes from HEK293T cells expressing RCAN1 and Dyrk1A. As shown in supplemental Fig. S1, phosphorylation of RCAN1 was detected in the RCAN1-Dyrk1A immunocomplex but not in control immunocomplex kinase assays. These data support the conclusion that Dyrk1A phosphorylates RCAN1.

An examination of the amino acid sequence of RCAN1 revealed the presence of five potential Dyrk1A phosphorylation sites at Ser^{108}, Ser^{112}, Thr^{124}, Thr^{153}, and Thr^{192}, each of which is followed by a proline residue conserved in human, rat, and mouse sequences. To identify the specific RCAN1 residues phosphorylated by Dyrk1A, each potential RCAN1 phosphorylation site was replaced with alanine, resulting in S108A, S112A, T124A, T153A, T192A, and the double mutant S112A/T192A. Purified RCAN1 wild type and mutants were incubated

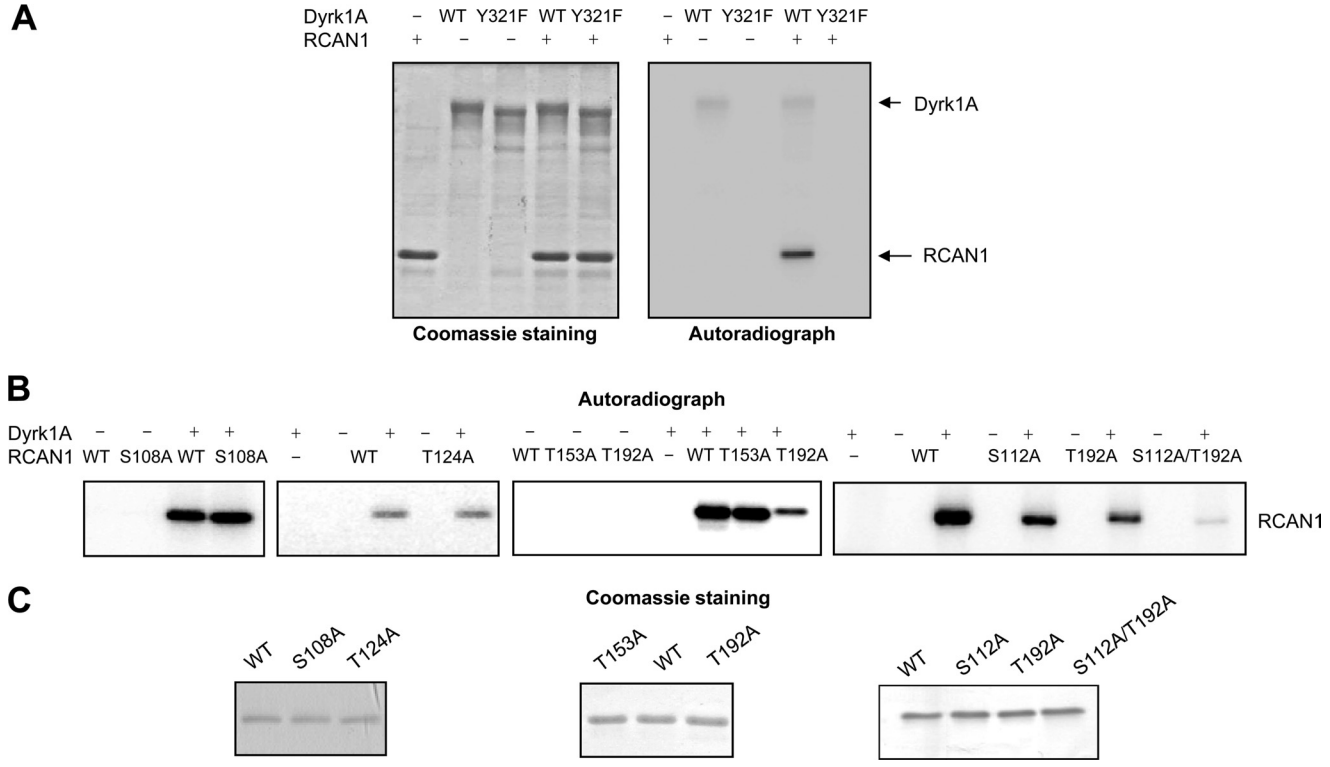

FIGURE 2. **Dyrk1A phosphorylates RCAN1 at Ser^{108} and Thr^{192} residues.** *A*, Coomassie staining of SDS-polyacrylamide gels containing purified recombinant Dyrk1A WT and Y321F and RCAN1 proteins (*left*). *WT*, wild type; *YF*, Y321F kinase-inactive mutant Dyrk1A. *Right*, autoradiograph of SDS-polyacrylamide gels containing the products of *in vitro* kinase assays performed using an RCAN1 substrate and Dyrk1A (WT and YF). Phsopho-RCAN1 and phospho-Dyrk1A (autophosphorylated forms) are indicated in the autoradiograph by *arrows*. *B*, autoradiograph of SDS-polyacrylamide gels containing the products of the *in vitro* kinase assays performed using RCAN1 substrates (WT and mutants) and Dyrk1A. Phsopho-RCAN1 bands are shown. *C*, Coomassie staining of SDS-polyacrylamide gels containing purified recombinant wild-type and mutant RCAN1 proteins.

with recombinant Dyrk1A in a kinase assay buffer containing [γ-^{32}P]ATP. This analysis revealed that mutation of serine 112 and threonine 192 to alanine strongly reduced the phosphorylation level of RCAN1. The S112A/T192A double mutation reduced the phosphorylation even further, whereas mutations at positions 108, 124, or 153 had little effect on Dyrk1A-dependent phosphorylation (Fig. 2*B*). As shown in Fig. 2*C*, the amounts of RCAN1 WT and mutants used in the kinase assay were similar. These results suggest that Dyrk1A selectively phosphorylates RCAN1 at Ser^{112} and Thr^{192} residues.

Phosphorylation of RCAN1 by Dyrk1A at Ser^{112} Primes the Protein for GSK3β-mediated Phosphorylation—Previous work showed that mitogen-activated protein kinase (MAPK) phosphorylates RCAN1 at serine 112 to prime it for subsequent phosphorylation at serine 108 by GSK3β (33). Dyrk1A occasionally plays a role as a GSK3β-priming kinase by phosphorylating the serine or threonine residue in target substrates located 4 amino acids downstream from the C terminus of another GSK3β-phosphorylated serine or threonine (4). Therefore, we anticipated that phosphorylation of Ser^{112} by Dyrk1A would prime for the phosphorylation of Ser^{108} by GSK3β. To investigate whether Dyrk1A could prime GSK3β-mediated phosphorylation of RCAN1, wild-type GST-RCAN1 protein bound to glutathione-Sepharose beads was prephosphorylated in the presence or absence of recombinant Dyrk1A. After the non-radioactive priming step, the bead-bound GST fusion proteins were washed extensively to remove recombinant Dyrk1A. Phosphorylated GST fusion proteins were then incubated with and without GSK3β in a kinase assay buffer containing [γ-^{32}P]ATP. Fig. 3*A* shows that RCAN1 prephosphorylated by Dyrk1A was strongly phosphorylated by GSK3β, although GSK3β and residual Dyrk1A alone slightly phosphorylated RCAN1.

We performed GSK3β mutation analysis to determine if Dyrk1A primes for phosphorylation at Ser^{108} of RCAN1. GST-RCAN1 proteins, either wild-type or mutant forms (S108A, S112A, or T192A), bound to glutathione-Sepharose beads were first phosphorylated using recombinant Dyrk1A in the presence or absence of non-radioactive ATP. Phosphorylated GST fusion proteins were then incubated with GSK3β in a kinase assay buffer containing [γ-^{32}P]ATP. As shown in Fig. 3*B*, Dyrk1A can prime wild-type RCAN1 for subsequent phosphorylation by GSK3β only in the presence of ATP. RCAN1 phosphorylation by GSK3β did not occur with proteins carrying mutations at S108A and S112A, which are the sites of GSK3β and Dyrk1A phosphorylation, respectively. In the priming experiment with the T192A mutant, the Dyrk1A-prephosphorylated RCAN1 was as strongly phosphorylated by GSK3β as was the wild-type RCAN1, excluding the possibility of non-canonical GSK3 priming (the priming kinase phosphorylates a residue required for GSK3β phosphorylation not at the +4-position), which has been shown for mammalian Dyrk1A kinase on NFAT (5) and for the Dyrk1A orthologue MBK-2 in *Caenorhabditis elegans* (34). These results suggest that Dyrk1A-mediated phosphorylation of Ser^{112} primes RCAN1

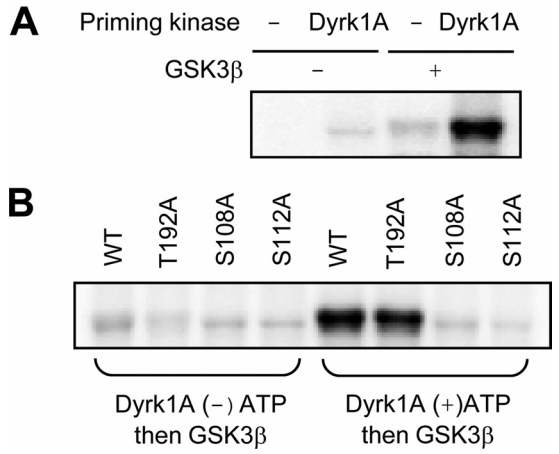

FIGURE 3. **Phosphorylation of RCAN1 at Ser^{112} by Dyrk1A primes for Ser^{108} phosphorylation by GSK3β.** *A*, wild-type GST-RCAN1 protein bound to glutathione-Sepharose beads was phosphorylated in the presence (Dyrk1A) or absence (−) of Dyrk1A, washed, and subjected to phosphorylation in the presence (+) or absence (−) of GSK3β and [γ-^{32}P]ATP. *B*, GST-RCAN1 proteins, either wild-type or mutant forms (S108A, S112A, or T192A), bound to glutathione-Sepharose beads were phosphorylated by Dyrk1A in the presence (+) or absence (−) of non-radioactive ATP, washed, and subjected to phosphorylation by GSK3β and [γ-^{32}P]ATP.

for subsequent phosphorylation by GSK3β at Ser^{108} *in vitro*, supporting a role for Dyrk1A as a priming kinase for GSK3β.

Phosphorylation at Thr^{192} by Dyrk1A Enhances the Activity of RCAN1 as a Caln Inhibitor—The effect of Dyrk1A-mediated phosphorylation of RCAN1 on the activity of RCAN1 as an inhibitor of Caln was examined. Prior to performing the Caln activity assay, purified GST-RCAN1 bound to glutathione-Sepharose beads was incubated with and without Dyrk1A in the presence and absence of 10 mM non-radioactive ATP for 90 min at 30°C, and the bead-bound GST-RCAN1 was washed extensively to remove recombinant kinase and ATP. As shown in Fig. 4*A*, RCAN1 phosphorylated by Dyrk1A inhibited Caln activity by 59%, whereas nonphosphorylated RCAN1 without ATP and without Dyrk1A inhibited Caln activity by 52 and 53%, respectively. In five independent experiments, the phosphorylation of RCAN1 enhanced its ability to inhibit Caln phosphatase activity by 27 ± 6% relative to that of nonphosphorylated RCAN1 without ATP ($p < 0.05$) and by 14 ± 3% relative to that of nonphosphorylated RCAN1 without Dyrk1A ($p < 0.05$) (Fig. 4*A*, *right*), suggesting that Dyrk1A-mediated phosphorylation of RCAN1 enhances its ability to inhibit Caln.

The effect of Ser^{112} and Thr^{192} phosphorylation on RCAN1 inhibition of Caln was assessed using RCAN1 WT and the S112A and T192A mutants. We first performed RCAN1 dosage-dependent Caln assays and found that RCAN1 inhibits Caln activity in a dose-dependent manner (supplemental Fig. S2*A*). We used 0.8 or 1.6 μg of RCAN1 WT and the phosphorylation-defective mutants in Fig. 4*B* with similar results at both concentrations. Both RCAN1 WT and RCAN1(S112A) inhibited Caln activity by 55%, whereas RCAN1(T192A) inhibited Caln activity by 51% (Fig. 4*B*). In six independent experiments, the RCAN1(S112A) and RCAN1(T192A) mutants exhibited reduced inhibition of Caln phosphatase activity (3 ± 1% ($p < 0.05$) and 9 ± 1% ($p < 0.001$), respectively) relative to that of RCAN1 WT (Fig. 4*B*, *right*). These results suggest that RCAN1 inhibition of Caln activity is mostly regulated by Dyrk1A-mediated phosphorylation of RCAN1 at Thr^{192}, although there could be a small contribution by phosphorylation at Ser^{112}.

A previous report showed that RCAN1 inhibited NFAT transcriptional activity in a dose-dependent manner in HEK293T cells, and Dyrk1A showed a synergistic effect with RCAN1 in blocking NFAT-dependent transcription in cortical neurons (25). The effect of RCAN1 WT and the S112A and T192A mutants on NFAT transcriptional activity was therefore investigated. We first determined the dosage dependence of RCAN1 in NFAT assays and found that RCAN1 inhibits NFAT transcriptional activity in a dose-dependent manner (supplemental Fig. S2*B*). In HEK293T cells, RCAN1 WT inhibited NFAT transcriptional activity by 61%, whereas the RCAN1(S112A) and RCAN1(T192A) mutants inhibited NFAT-dependent transcription by 60 and 53%, respectively (Fig. 4*C*, *left*). The expression of RCAN1 WT and mutants was similar (Fig. 4*C*). In 11 independent experiments, the RCAN1(T192A) mutant showed a 10 ± 2% reduction in the ability to inhibit NFAT-dependent transcription in comparison with RCAN1 WT ($p < 0.001$) (Fig. 4*C*, *right*). These results suggest that Dyrk1A-mediated phosphorylation of RCAN1 at Thr^{192} regulates the transcriptional activity of NFAT, possibly through the inhibition of Caln activity.

The finding that the overexpression of RCAN1 caused the hyperphosphorylation of Tau (35), and our previous observation that Dyrk1A phosphorylated Tau at Thr^{212} and Ser^{404} residues prompted us to examine the effect of RCAN1 and Caln on Tau phosphorylation. Western blot analysis was performed with lysates of HEK293T cells that had been transiently transfected with a Tau expression plasmid, either in the presence or absence of a plasmid encoding RCAN1 or Caln A. Phosphorylation of Thr^{212} and Ser^{404} residues was detected with phospho-Thr^{212}-Tau (p-Tau212)-specific and phospho-Ser^{404}-Tau (p-Tau404)-specific antibodies, respectively. Although the amounts of Tau were similar, the amounts of p-Tau212 and p-Tau404 were increased in cells expressing RCAN1 but decreased in cells expressing Caln (Fig. 4*D*), suggesting that these Tau residues are dephosphorylated by Caln. To further examine whether the expression of p-Tau212 and p-Tau404 is sensitive to Caln, HEK293T cells expressing Tau and Caln were treated with a Caln inhibitor, FK506 (1 μM). As shown in supplemental Fig. S3, the amounts of p-Tau212 and p-Tau404 were decreased in cells expressing Caln but recovered in cells treated with FK506, supporting the conclusion that p-Tau212 and p-Tau404 are dephosphorylated by Caln.

Examination of the effect of RCAN1 WT and the S112A and T192A mutants on Tau phosphorylation revealed that the RCAN1(T192A) mutant reduced the phosphorylation of Tau at Thr^{212} and Ser^{404} residues compared with RCAN1 WT (Fig. 4*E*). The effect of RCAN1(S112A) on these Tau residues was nearly the same as that of RCAN1 WT (Fig. 4*E*). In six independent experiments, the RCAN1(T192A) mutant inhibited Tau phosphorylation at Thr^{212} and Ser^{404} by 55 ± 5% and 36 ± 8%, respectively, relative to RCAN1 WT ($p < 0.01$) (Fig. 4*F*). These results suggest that the increased phosphorylation of Tau mediated by the inhibition of its dephosphorylation by Caln is regulated by Dyrk1A-mediated phosphorylation of RCAN1 at Thr^{192}.

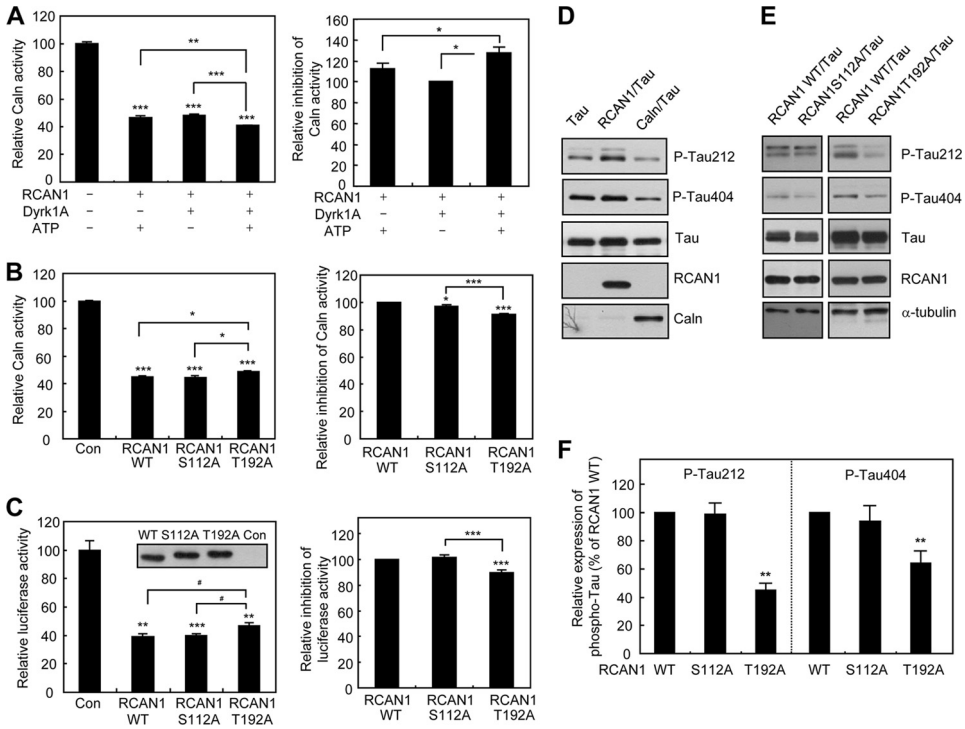

FIGURE 4. **Phosphorylation of RCAN1 at Thr^{192} by Dyrk1A enhances its ability to inhibit Caln.** *A*, purified GST-RCAN1 bound to glutathione-Sepharose beads was incubated with and without Dyrk1A in the presence and absence of non-radioactive ATP, washed, and assessed for its activity as an inhibitor of Caln as described under "Experimental Procedures." The control (−*RCAN1*, −*Dyrk1A*, −*ATP*) contained the assay buffer and Caln/CaM. The results shown in the *left panel* are representative experiments performed in triplicate, and Caln activity is plotted as the percentage of that of the control. In the *right panel*, the inhibition of Caln activity by phospho-RCAN1 or a control of RCAN1 without Dyrk1A is plotted as the percentage of that of nonphospho-RCAN1 (−*ATP*). Data are presented as the mean ± S.E. (*error bars*) of six independent experiments, each performed in triplicate. *B*, Caln activity assays using purified recombinant Caln with and without purified recombinant His-tagged RCAN1 WT or S112A or T192A mutant. The results shown in the *left panel* are of representative experiments performed in triplicate, and Caln activity is plotted as the percentage of that of the control. In the *right panel*, inhibition of Caln activity by RCAN1(S112A and T192A) is plotted as the percentage of that of RCAN1 WT. Data are presented as the mean ± S.E. of six independent experiments. *C*, the *left panel* shows representative experiments performed in triplicate. Luciferase activity is plotted as the percentage of that of the control. In the *right panel*, inhibition of luciferase activity by RCAN1 mutants is plotted as the percentage of that of RCAN1 WT. Data are presented as the mean ± S.E. of seven (S112A) or 11 (T192A) independent experiments. Immunoblotting with an anti-Myc antibody of extracts from HEK293T cells transfected with indicated plasmid is shown *inside* the *graph* in the *left panel*. *D* and *E*, representative immunoblots of HEK293T cells co-transfected with a plasmid encoding Tau and the indicated plasmid or a control pcDNA3.1 and analyzed with p-Tau212, p-Tau404, Tau, RCAN1, Caln, and α-tubulin antibodies. *F*, densitometric analysis of the immunoblots normalized with respect to the Tau and RCAN1 signals. The amount of p-Tau212 and p-Tau404 from HEK293T cells transfected with RCAN1(S112A) and RCAN1(T192A) is plotted as the percentage of that of RCAN1 WT. Data are shown as means ± S.E. of six independent experiments. #, $p < 0.07$; *, $p < 0.05$; **, $p < 0.01$; ***, $p < 0.001$ *versus* the control or RCAN1 WT if not indicated otherwise (Student's *t* test).

Dyrk1A-mediated Phosphorylation of RCAN1 Increases Binding of RCAN to Caln—Because the C-terminal region of RCAN1 is reported to bind to Caln (29, 36, 37), we tested whether the effect of Dyrk1A-mediated phosphorylation of RCAN1 on its ability to inhibit Caln activity is linked to its ability to bind Caln. Purified GST-RCAN1 bound to glutathione-Sepharose beads was incubated with Dyrk1A in the presence and absence of 10 mM non-radioactive ATP for 1 h at 37 °C, and the bead-bound GST fusion proteins were washed to remove recombinant kinase and ATP prior to performing the binding assay. As shown in Fig. 5*A*, RCAN1 phosphorylated by Dyrk1A showed enhanced binding to Caln compared with non-phosphorylated RCAN1. In six independent experiments, the binding of phosphorylated RCAN1 to Caln was enhanced by 16 ± 6% relative to nonphosphorylated RCAN1 ($p < 0.05$) (Fig. 5*A*). To examine the role of Ser^{112} and Thr^{192} phosphorylation in the binding of RCAN1 to Caln, the interaction between Caln and either GST-RCAN1 WT or the phosphorylation-defective mutant was compared using a GST pull-down assay. As shown in Fig. 5*B*, the GST-RCAN1, but not GST, was able to bind to Caln overexpressed in HEK293T cell lysates, and the RCAN1(T192A) mutant showed inhibited Caln binding compared with that of RCAN1 WT. There was little difference between RCAN1 WT and RCAN1(S112A) in their effect on Caln binding. In 16 independent experiments, the binding of the RCAN1 T192A mutant to Caln was reduced by 13 ± 4% relative to the RCAN1 WT ($p < 0.01$) (Fig. 5*B*). These results suggest that Dyrk1A-mediated phosphorylation enhances the ability of RCAN1 to inhibit Caln, potentially through increased binding to Caln.

We then determined whether a similar effect of Dyrk1A-mediated phosphorylation is observed with the 57 C-terminal amino acids of RCAN1 (RCAN1Ct) composed of exon 7. As shown in supplemental Fig. S4, RCAN1Ct phosphorylated by Dyrk1A showed enhanced binding to Caln in comparison with nonphosphorylated RCAN1. In 4–9 independent experiments, the binding of phosphorylated RCAN1 to Caln was enhanced by 19 ± 4% relative to nonphosphorylated RCAN1 without Dyrk1A ($p < 0.05$) and by 12 ± 5% relative to nonphosphorylated RCAN1 without ATP ($p < 0.05$) (supplemental Fig. S4, *A* and *B*). When the interaction between Caln and either GST-RCAN1Ct WT or the T192A mutant was compared using a

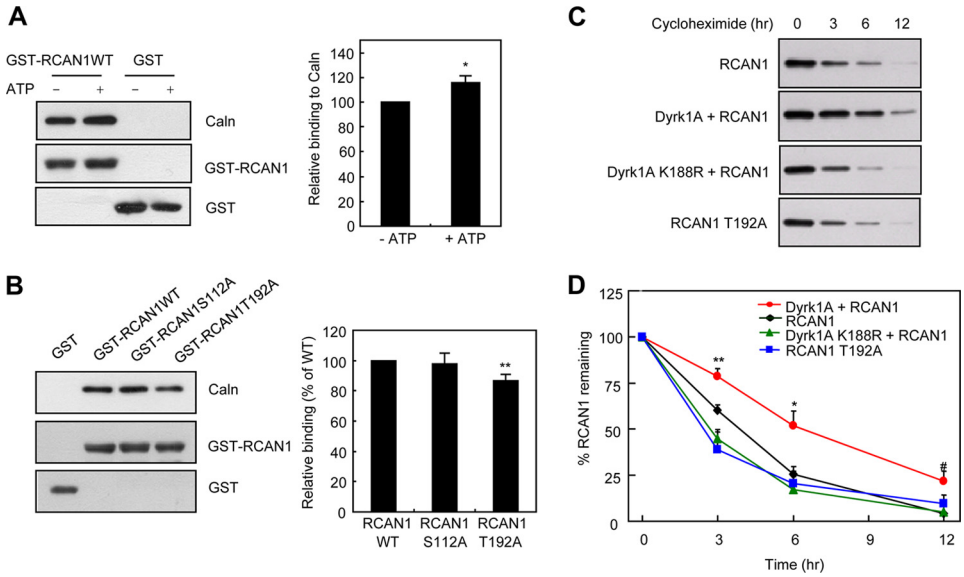

FIGURE 5. **Dyrk1A-mediated phosphorylation of RCAN1 increases binding of RCAN to Caln and leads to extended half-life.** *A*, purified GST or GST-RCAN1 bound to glutathione-Sepharose beads were incubated with Dyrk1A in the presence (+*ATP*) and absence (−*ATP*) of non-radioactive ATP, washed, and then incubated with HEK293T cell lysates transfected with a plasmid encoding Caln and subjected to immunoblot analyses of Caln and GST. The result shown in the *left panel* is a representative immunoblot. In the *right panel*, the densitometric analysis of the immunoblots was normalized to the GST-RCAN1 signals. Data are presented as the mean ± S.E. (*error bars*) of six independent experiments. *, $p < 0.05$ *versus* the nonphospho-RCAN1 (−*ATP*) (Student's *t* test). *B*, purified GST or GST-RCAN1 (or mutants) bound to glutathione-Sepharose beads were incubated with HEK293T cell lysates transfected with a plasmid encoding Caln and then subjected to immunoblotting for Caln and GST. The results shown in the *left panel* are representative immunoblots. In the *right panel*, the densitometric analysis of the immunoblots was normalized to the GST-RCAN1 signals. Data are presented as the mean ± S.E. of 10 (S112A) or 16 (T192A) independent experiments. **, $p < 0.01$ *versus* RCAN1 WT (Student's *t* test). *C*, HEK293T cells were transfected with the plasmid(s) indicated to the *left* of the blot. After 24 h, the cells were treated with 90 μM cycloheximide for the indicated times (0, 3, 6, and 12 h) and subjected to SDS-PAGE. Representative immunoblots of cell lysates with anti-Myc antibodies are shown. *D*, densitometric analysis of RCAN1 (normalized by α-tubulin) immunoblots. Each signal was plotted as the percentage of 0 h signal, and data are presented as means ± S.E. of four independent experiments. *, $p < 0.05$; **, $p < 0.01$ *versus* the other three groups; #, $p < 0.05$ *versus* two groups (RCAN1 and Dyrk1A K188R + RCAN1) each by Student's *t* test.

GST pull-down assay, the RCAN1Ct(T192A) mutant showed inhibited Caln binding compared with that of RCAN1Ct WT. In five independent experiments, the binding of the RCAN1 T192A mutant to Caln was reduced by 32 ± 9% relative to the RCAN1Ct WT ($p < 0.05$) (supplemental Fig. S4*C*). These results support the hypothesis that Dyrk1A-mediated phosphorylation at Thr^{192} enhances the ability of RCAN1 to bind to Caln, resulting in the inhibition of Caln activity.

Dyrk1A-mediated Phosphorylation of RCAN1 Leads to an Extended Half-life—In a previous study, Lee *et al.* (38) reported that the NF-κB-inducing kinase-mediated phosphorylation of the RCAN1 C-terminal region, spanning amino acids 90–197, increased the half-life of RCAN1. We examined whether Dyrk1A-mediated phosphorylation affects the protein stability of RCAN1. HEK293T cells were transfected with a plasmid encoding Myc-tagged RCAN1 alone or together with either WT Dyrk1A or the kinase-inactive mutant K188R or transfected with a plasmid encoding the Myc-tagged RCAN1(S112A or T192A) mutant alone or together with Dyrk1A as indicated in the legend to Fig. 5*C* and supplemental Fig. S5. The transfected cells were incubated with cycloheximide, a protein synthesis inhibitor, for the indicated time, and the expression level of RCAN1 was measured by Western blot analysis using an anti-Myc antibody (Fig. 5*C*). Compared with the half-life of RCAN1 in cells expressing RCAN1 alone or together with Dyrk1A K188R, the half-life of RCAN1 expressed with Dyrk1A WT was significantly increased (Fig. 5, *C* and *D*).

The half-life of RCAN1(T192A) was slightly shortened compared with that of RCAN1 WT and was not affected by co-expression with Dyrk1A (Fig. 5, *C* and *D*, and supplemental Fig. S5*A*). The half-life of the S112A mutant of RCAN1 was similar to or a little shorter than that of RCAN1 WT (supplemental Fig. S5*B*). The half-life of the S112A mutant was extended by Dyrk1A co-expression (supplemental Fig. S5*C*). These results suggest that Dyrk1A-mediated phosphorylation at Thr^{192} extends the half-life of RCAN1, potentially contributing to the enhanced ability of RCAN1 to inhibit Caln.

Phospho-Thr^{192}-RCAN1 (pT192-RCAN1) Is Increased in Dyrk1A TG Mice—To further explore the link between Dyrk1A and RCAN1 through the phosphorylation of RCAN1 at Thr^{192} *in vivo*, the brains of transgenic mice overexpressing the human Dyrk1A protein (Dyrk1A TG mice) were analyzed. A rabbit polyclonal antibody to the phosphopeptide $RPEYT^{192}(PO_4)PIHLS$ was generated and affinity-purified. To determine the specificity of the phosphospecific RCAN1 (pT192-RCAN1) antibody, Western blot analysis was performed with lysates of HEK293T cells that had been transiently transfected with RCAN1 WT or RCAN1(T192A) expression plasmids either alone or in the presence of plasmids encoding Dyrk1A. The phosphospecific antibody was able to detect the phospho-RCAN1 band only in the presence of both RCAN1 WT and Dyrk1A (Fig. 6*A*). The specificity of the pT192-RCAN1 antibody was further demonstrated by peptide competition experiments showing that the antibody signal in Western blots of mouse brain lysates was blocked by preincubation with the RCAN1-phosphopeptide but not with the RCAN1-nonphosphopeptide (Fig. 6*B*). When mouse brain lysates were treated with λ-protein phosphatase and Western blotting was

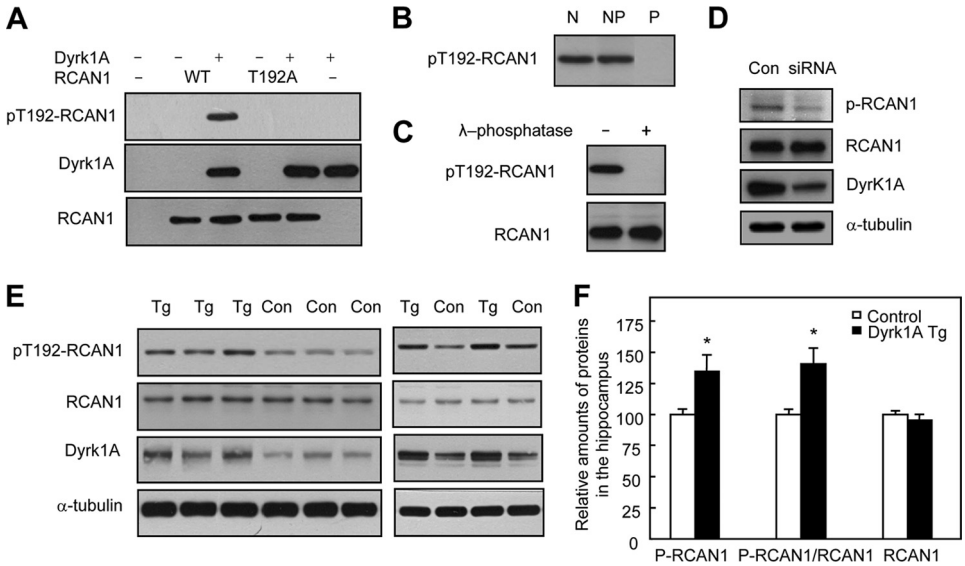

FIGURE 6. **Phospho-Thr^{192}-RCAN1 is increased in Dyrk1A TG mice.** *A*, HEK293T cells transfected with the indicated plasmid(s) or control vector (−) were analyzed by immunoblots with pT192-RCAN1, Dyrk1A, or RCAN1 antibodies. *B*, peptide competition assay for the pT192-RCAN1 antibody. Mouse brain lysates were analyzed by immunoblot with the pT192-RCAN1 antibody preincubated in the absence (*N*) or the presence of RCAN1-nonphosphopeptide (*NP*) or RCAN1-phosphopeptide (*P*). *C*, mouse brain lysates were treated with (+) or without (−) λ-protein phosphatases and subsequently analyzed by immunoblot with the pT192-RCAN1 or RCAN1 antibodies. *D*, PC12 cells were transfected with control (*Con*) or Dyrk1A (*siRNA*) siRNAs. The levels of Dyrk1A, phospho-RCAN1, RCAN1, and α-tubulin were examined by immunoblot analyses. *E*, representative immunoblots of hippocampal lysates of 3-week-old (*left*) or 4-week-old (*right*) Dyrk1A TG mice and control littermates. The RCAN1–1 isoform is shown. *F*, densitometric analysis of pT192-RCAN1 signals in the immunoblots was either normalized by α-tubulin (*P-RCAN1*) or RCAN1 (*P-RCAN1/RCAN1*) signals. The RCAN1 level was normalized by α-tubulin (*RCAN1*). Phospho-RCAN1 amounts of Dyrk1A TG mice are plotted as the percentage of those of wild-type control littermates. Data are represented as means ± S.E. (*error bars*). *, $p < 0.05$ *versus* littermate controls by Student's *t* test.

performed with the pT192-RCAN1 antibody, the antibody signal disappeared, confirming that the phosphospecific RCAN1 antibody recognizes the phosphorylated forms of RCAN1 (Fig. 6*C*).

To determine whether Dyrk1A phosphorylates RCAN1 at Thr^{192} in cells, PC12 cells were transfected with Dyrk1A-specific siRNA. An ineffective Dyrk1A siRNA was used as a negative control. After 48–72 h of siRNA treatment, Dyrk1A siRNA reduced the endogenous Dyrk1A expression (Fig. 6*D*). Correspondingly, the level of phospho-Thr^{192}-RCAN1 was also reduced, whereas the expression of RCAN1 was similar for the siRNA-transfected cells. This result suggests that Dyrk1A is the kinase responsible for phosphorylating RCAN1 at Thr^{192}.

To determine whether the expression of phospho-RCAN1 is increased in Dyrk1A TG mice, immunoblot analyses were performed with brain lysates prepared from the hippocampus of Dyrk1A TG mice and the control littermates (Fig. 6*E*). When compared with the control littermates, Dyrk1A TG mice show a 1.5–2-fold increase in Dyrk1A activity and expression in the hippocampus (10). The level of phospho-RCAN1 (normalized by α-tubulin) in the Dyrk1A TG mice was increased by 34 ± 13% ($p < 0.05$) in the hippocampus relative to that of the controls. After normalization to the levels of total RCAN1, the amount of phospho-RCAN1 in the Dyrk1A TG mice was increased by 41 ± 13% ($p < 0.05$) in the hippocampus, compared with that of the controls; in contrast, the amount of RCAN1 itself did not differ significantly between Dyrk1A TG and control littermate mice (Fig. 6*F*). These results demonstrate that the levels of phospho-RCAN1 are enhanced when Dyrk1A levels are increased, suggesting that overexpression of Dyrk1A may be functionally linked to RCAN1 activity *in vivo* through phosphorylation.

RCAN1 Partially Colocalizes with Dyrk1A—To determine whether endogenous Dyrk1A and RCAN1 co-localize in the cell, double immunocytochemistry was performed on NGF-differentiated PC12 cells and primary rat neuronal cells. Dyrk1A and RCAN1 proteins are primarily found in the cytoplasm, although Dyrk1A and RCAN1 staining are also present in the nucleus (Fig. 7, *A* and *B*). In the *merged image*, Dyrk1A was partially co-localized with RCAN1 in the cytosol, in the nucleus, and near the end of the neuron-like processes in NGF-treated PC12 cells (Fig. 7*A*) or synaptic boutons in the primary neuronal cells (Fig. 7*B*), suggesting that Dyrk1A potentially phosphorylates RCAN1 in these areas.

We then examined the expression of endogenous phospho-RCAN1. The specificity of the pT192-RCAN1 antibody was demonstrated by peptide competition experiments showing that the antibody signal of NGF-differentiated PC12 cells was completely blocked by preincubation with the RCAN1-phosphopeptide, but not with the RCAN1-nonphosphopeptide (Fig. 7*C*). Notably, the phospho-RCAN1 antibody labeled the neuritic terminals and nuclei of NGF-differentiated PC12 cells (Fig. 7, *C* and *D*) and synaptic boutons in the primary neuronal cells (Fig. 7*E*), consistent with a *merged image* of Dyrk1A and RCAN1 staining (Fig. 7, *A* and *B*). This finding was further supported by the co-localization of RCAN1 and pT192-RCAN1 (supplemental Fig. S6).

DISCUSSION

In the present study, we demonstrate for the first time that Dyrk1A interacts with and phosphorylates RCAN1 at Ser^{112} and Thr^{192} residues (Figs. 1 and 2). The phosphorylation of RCAN1 at Ser^{112} by Dyrk1A primes the protein for GSK3β-mediated phosphorylation at Ser^{108} (Fig. 3). Phosphorylation of

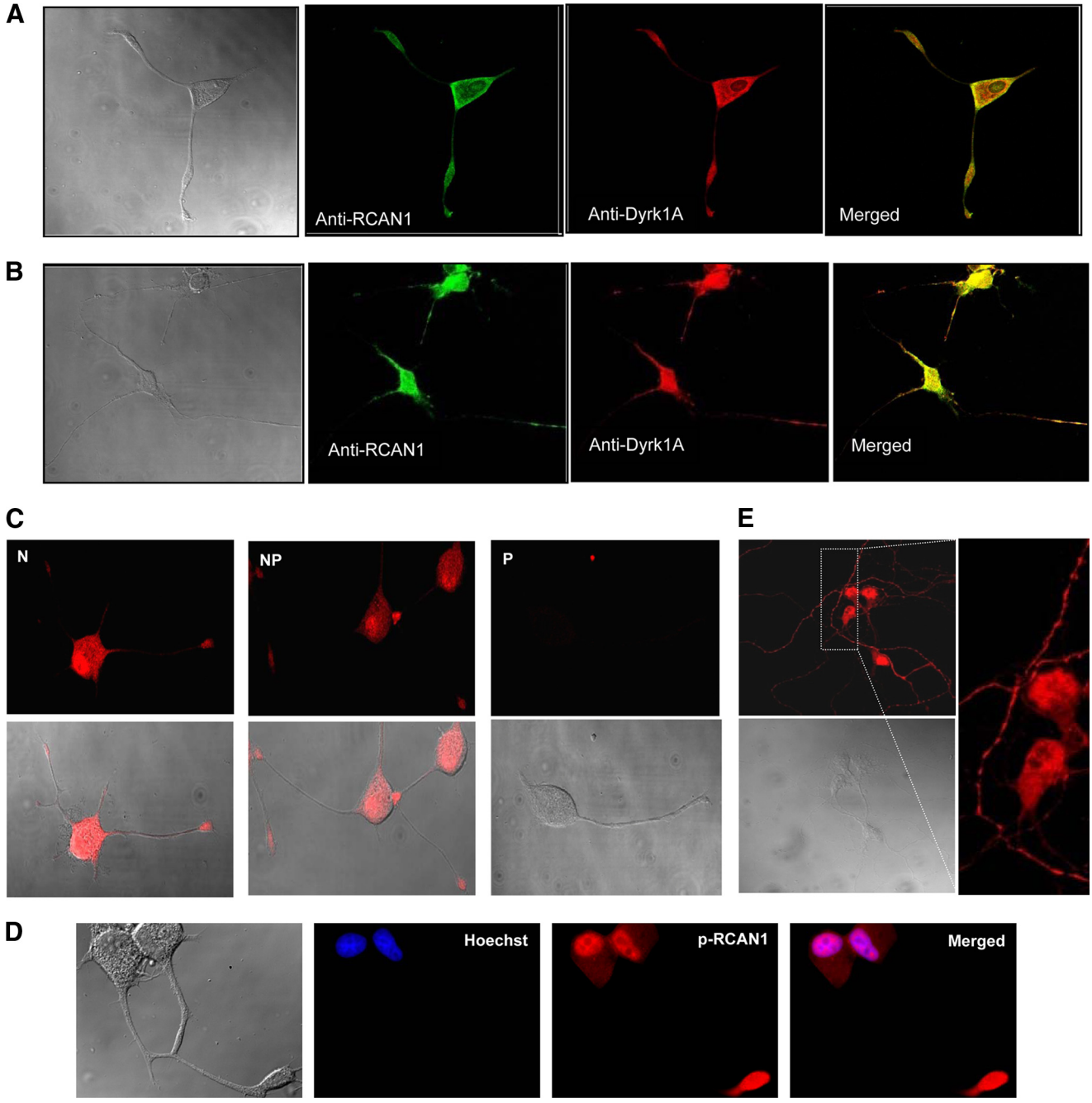

FIGURE 7. **Dyrk1A partially colocalizes with RCAN1.** NGF-differentiated PC12 cells (*A*) or rat primary cortical neuronal cells (*B*) were processed for double immunofluorescence. Rabbit anti-Dyrk1A antibody and mouse anti-RCAN1 antibody was used to detect endogenous Dyrk1A, RCAN1, and Dyrk1A + RCAN1 (merged). The phase image of the field is on the *left*. *C*, peptide competition for phospho-RCAN1 antibody by the immunocytochemistry. NGF-differentiated PC12 cells were processed for immunofluorescence with phospho-RCAN1 antibody preincubated in the absence (*N*) or the presence of RCAN1-nonphosphopeptide (*NP*) or RCAN1-phosphopeptide (*P*). The cells were then incubated with Texas Red goat anti-rabbit antibodies. The *bottom panels* show merged phase and fluorescence images. *D*, after the phospho-RCAN1 antibody treatment, NGF-differentiated PC12 cells were incubated with Texas Red goat anti-rabbit antibodies. For nuclear staining, Hoechst 33342 stain (*Hoechst*) was added to the cells. *E*, rat primary cortical neuronal cells were processed for immunofluorescence with phospho-RCAN1 antibody. The regions within the *rectangular areas* are *enlarged*.

RCAN1 at Thr^{192} by Dyrk1A increases its activity as an inhibitor of Caln, resulting in reduced NFAT transcriptional activity and enhanced Tau phosphorylation (Fig. 4). These results can be attributed to the enhanced binding of RCAN1 to Caln and slower degradation of phospho-RCAN1 (Fig. 5). Furthermore, the levels of phospho-RCAN1 were enhanced in the brains of Dyrk1A TG mice, providing *in vivo* evidence of the phosphorylation of RCAN1 by Dyrk1A (Fig. 6). These results suggest a direct regulatory association between Dyrk1A and RCAN1 in the Caln-NFAT signaling and Tau hyperphosphorylation pathways.

Mammalian RCAN1 contains five conserved sites for Dyrk1A-mediated phosphorylation at Ser^{108}, Ser^{112}, Thr^{124}, Thr^{153}, and Thr^{192}, all of which precede a proline residue. Ser^{108} and Ser^{112} are located within the highly conserved FLISPP*X*SPP sequence motif. The results of the present study

showed that Dyrk1A phosphorylates RCAN1 at Ser^{112} and Thr^{192} residues. An immunofluorescence study showed that a phospho-Thr^{192} RCAN1 antibody labeled the synaptic boutons in primary neuronal cells as well as neuritic terminals and the nuclei of NGF-differentiated PC12 cells and primary neuronal cells (Fig. 7), suggesting that Dyrk1A participates in the phosphorylation of RCAN1 in these regions. Recent reports showed that 12% of brain Dyrk1A is localized to the nucleus, 78% is associated with an insoluble cytoskeletal fraction, and 10% is associated with a soluble cytoplasmic fraction (39, 40). RCAN1 is present in both the cytosol and the nucleus, and the last 33 C-terminal residues of RCAN1 are reported to be necessary for its nuclear localization (41). The predominant nuclear localization of phospho-Thr^{192} RCAN1 detected in this study is consistent with these reports and suggests that phosphorylation at Thr^{192} is potentially important for the nuclear localization of RCAN1 (Fig. 7, *C*–*E*).

The effect of RCAN1 on Caln-NFAT signaling depends on post-translational modification, such as phosphorylation. A previous study identified the C-terminal 57 residues of RCAN1 that are required to bind Caln with high affinity and that inhibit Caln activity with a potency similar to that of full-length RCAN1 (37). The highly conserved FLISPP*X*SPP sequence motif is apparently not critical for Caln binding and inhibition, as shown by mutants of RCAN1 with amino acid substitutions within the conserved motif (37, 42), although there is controversy as shown below. Consistent with these reports, we observed that Dyrk1A-mediated phosphorylation of RCAN1 at Thr^{192} enhanced its binding to Caln (Fig. 5, *A* and *B*), and there was little difference between RCAN1(S112A) mutant and RCAN1 WT in terms of their effect on Caln binding and activity. Different residues of RCAN1 are phosphorylated by various kinases, including GSK3β, MAPK, BMK1, NF-κB-inducing kinase, and TGF-β-activated kinase 1 (TAK1) (33, 38, 43, 44). BMK1-mediated phosphorylation of RCAN1 causes dissociation of RCAN1 from Caln (44), whereas the phosphorylation of the C-terminal region of RCAN1 by NF-κB-inducing kinase increases the stability of the protein (38). Phosphorylation of RCAN1 at Ser^{112} by MAPK primes the protein for the subsequent phosphorylation by GSK3β at Ser^{108} (33). Phosphorylation of Ser^{108} by GSK3β suppresses the inhibitory activity of RCAN1 and converts the protein into an activator of Caln (45). Phosphorylation of RCAN1 at Ser^{94} and Ser^{136} residues by TAK1 also switches RCAN1 from an inhibitor to a facilitator of Caln-NFAT signaling, enhancing NFATc1 nuclear translocation (43). The exact mechanism of this facilitative property of RCAN1 has not yet been demonstrated. Dyrk1A-mediated phosphorylation of RCAN1 at Thr^{192} activates its function as a Caln inhibitor, resulting in reduced NFAT transcriptional activity, and slows degradation of RCAN1 (Figs. 4 and 5). In contrast, phosphorylation of RCAN1 at Ser^{112} by Dyrk1A (Fig. 3) may switch its function to a Caln activator by priming for GSK3β-mediated phosphorylation at Ser^{108}. Although the phosphorylation of RCAN1 by various kinases could serve as a potential mechanism, it remains uncertain how endogenous RCAN1 acts as inhibitor or facilitator of Caln.

Several reports have shown that the ability of RCAN to inhibit Caln phosphatase activity requires the interaction between RCAN protein and the Caln A subunit (29, 46, 47). Therefore, increased ability of RCAN1 to inhibit the Caln activity (Fig. 4) may be a secondary effect of the enhanced interaction between them through Dyrk1A-mediated phosphorylation at Thr^{192} (Fig. 5, *A* and *B*, and supplemental Fig. S4). A Val-rich region in the C-terminal part of RCAN1 is involved in the interaction (36, 37, 48, 49), and most C-terminal amino acids (where Thr^{192} is located) are not required (48). In contrast, a 38-residue fragment of RCAN1–1 without the Val-rich region (residues 215–252) was able to bind Caln when overexpressed in a mammalian cell line (50). Furthermore, RCAN1 inhibition of Caln activity is mediated by the C-terminal 30 residues of RCAN1-1, which acts in *cis* with the docking motif (36). The differences between RCAN1 WT and the T192A mutant in their effect on Caln binding and activity are minute although statistically significant (Figs. 4 and 5 and supplemental Fig. S4). Perhaps this small effect was missed in a previous study (48). The extended half-life caused by Dyrk1A-mediated phosphorylation may also contribute to RCAN1 inhibition of Caln activity. Phosphorylation of RCAN1 by Dyrk1A may fine tune RCAN1 for effective control over Caln activity and can therefore act as a regulator of Caln-dependent cellular pathways.

In DS fetal brains, Caln activity is lower than in normal subjects (22), and NFAT hyperphosphorylated species were found to be increased (25). These findings can be explained by a cooperative effect of overexpressed RCAN1 and Dyrk1A, which are located on chromosome 21, on Caln/NFAT signaling, although DS is certainly more than a disturbance of NFAT signaling (42). Dyrk1A phosphorylates several residues of the microtubule-associated protein Tau, including Thr^{212} and Ser^{404} (11). Tau is dephosphorylated by Caln (51), which is the target of RCAN1, as also shown in Fig. 4*D* and supplemental Fig. S3 of this work. Our finding that Dyrk1A-mediated phosphorylation of RCAN1 at Thr^{192} enhances Tau phosphorylation, as shown in Fig. 4, *E* and *F*, suggests that overexpression of Dyrk1A and RCAN1 in DS may lead to an increase in Tau hyperphosphorylation, contributing to the early onset of the pathological features of AD in DS patients. The connection between RCAN1/Dyrk1A and Caln/NFAT signaling in the pathogenesis of AD seems more complicated. Dyrk1A mRNA expression was elevated in the hippocampus of AD patients (12), and Dyrk1A immunoreactivity was increased in the frontal cortex, entorhinal cortex, and hippocampus of AD patients (27). In addition, mRNA levels of RCAN1 are also much higher in the brains of patients with AD (28). Elevated levels of activated Caln have been reported in people with mild cognitive impairment and AD (52, 53), although there is controversy as to the activity of Caln in AD patients (54). In nuclear fractions of post-mortem hippocampal tissue, NFAT1 is selectively activated in mild cognitive impairment patients, whereas NFAT3 is activated in AD patients (52, 53). Upon activation by Caln, the NFAT transcription factor translocates from the cytosol to the nucleus and induces the expression of specific genes, including one of the *RCAN1* isoforms (55). Therefore, elevated RCAN1 levels in AD tissue are partially due to an increase in Caln/NFAT signaling. It remains to be elucidated whether increased Caln/NFAT signaling in AD patients can induce the expression of Dyrk1A. Although

RCAN1 is an endogenous Caln inhibitor, the phosphorylation by GSK3β and TAK1 converts RCAN1 into an activator of Caln (43, 45). Therefore, overexpressed RCAN1 may help attenuate or intensify Caln/NFAT signaling in AD through negative or positive feedback loops. Alternatively, the effect of RCAN1 on calcineurin signaling may depend on RCAN1 and Dyrk1A expression level in DS and AD brains. When RCAN1 and Dyrk1A are overexpressed at very high levels, as in DS brains, RCAN1 may act as an Caln inhibitor, whereas when RCAN1 and Dyrk1A are overexpressed at low to intermediate levels, as in AD brains, Dyrk1A may activate Caln-NFAT signaling through RCAN1, as suggested in the regulation of Caln activity by RCAN1 and TAK1 (43). Although we provide evidence that the RCAN1 activity as a Caln inhibitor is increased by Dyrk1A-mediated phosphorylation (Fig. 4) and pT192-RCAN1 level is enhanced in Dyrk1A TG brains (Fig. 6), *in vivo* significance of the RCAN1 phosphorylation in the pathogenesis of DS and AD is not clear. Further investigation will be necessary to determine whether RCAN1 activity from Dyrk1A TG brains is altered compared with that in control mouse brains and whether the pT192-RCAN1 level is indeed increased in the brains of DS and AD patients.

The results of the present study suggest that there is a direct regulatory link between Dyrk1A and RCAN1 in the Caln-NFAT signaling and Tau hyperphosphorylation pathways. Synergistic interactions between the chromosome 21 genes *RCAN1* and *Dyrk1A* might be responsible for a variety of pathological features associated with DS, including abnormal development, immune defects, and early onset of AD.

Acknowledgments—We thank Eun-Ah Song and Jung-Yeon Kwon for technical support in Western analysis.

REFERENCES

1. Becker, W., and Sippl, W. (2011) *FEBS J.* **278,** 246–256
2. Park, J., Oh, Y., and Chung, K. C. (2009) *BMB Rep.* **42,** 6–15
3. Park, J., Song, W. J., and Chung, K. C. (2009) *Cell Mol. Life Sci.* **66,** 3235–3240
4. Woods, Y. L., Cohen, P., Becker, W., Jakes, R., Goedert, M., Wang, X., and Proud, C. G. (2001) *Biochem. J.* **355,** 609–615
5. Gwack, Y., Sharma, S., Nardone, J., Tanasa, B., Iuga, A., Srikanth, S., Okamura, H., Bolton, D., Feske, S., Hogan, P. G., and Rao, A. (2006) *Nature* **441,** 646–650
6. Kentrup, H., Becker, W., Heukelbach, J., Wilmes, A., Schürmann, A., Huppertz, C., Kainulainen, H., and Joost, H. G. (1996) *J. Biol. Chem.* **271,** 3488–3495
7. Song, W. J., Sternberg, L. R., Kasten-Sportès, C., Keuren, M. L., Chung, S. H., Slack, A. C., Miller, D. E., Glover, T. W., Chiang, P. W., Lou, L., and Kurnit, D. M. (1996) *Genomics* **38,** 331–339
8. Guimerá, J., Casas, C., Pucharcòs, C., Solans, A., Domènech, A., Planas, A. M., Ashley, J., Lovett, M., Estivill, X., and Pritchard, M. A. (1996) *Hum. Mol. Genet.* **5,** 1305–1310
9. Shindoh, N., Kudoh, J., Maeda, H., Yamaki, A., Minoshima, S., Shimizu, Y., and Shimizu, N. (1996) *Biochem. Biophys. Res. Commun.* **225,** 92–99
10. Ryoo, S. R., Cho, H. J., Lee, H. W., Jeong, H. K., Radnaabazar, C., Kim, Y. S., Kim, M. J., Son, M. Y., Seo, H., Chung, S. H., and Song, W. J. (2008) *J. Neurochem.* **104,** 1333–1344
11. Ryoo, S. R., Jeong, H. K., Radnaabazar, C., Yoo, J. J., Cho, H. J., Lee, H. W., Kim, I. S., Cheon, Y. H., Ahn, Y. S., Chung, S. H., and Song, W. J. (2007) *J. Biol. Chem.* **282,** 34850–34857
12. Kimura, R., Kamino, K., Yamamoto, M., Nuripa, A., Kida, T., Kazui, H., Hashimoto, R., Tanaka, T., Kudo, T., Yamagata, H., Tabara, Y., Miki, T., Akatsu, H., Kosaka, K., Funakoshi, E., Nishitomi, K., Sakaguchi, G., Kato, A., Hattori, H., Uema, T., and Takeda, M. (2007) *Hum. Mol. Genet.* **16,** 15–23
13. Park, J., Yang, E. J., Yoon, J. H., and Chung, K. C. (2007) *Mol. Cell Neurosci.* **36,** 270–279
14. Ryu, Y. S., Park, S. Y., Jung, M. S., Yoon, S. H., Kwen, M. Y., Lee, S. Y., Choi, S. H., Radnaabazar, C., Kim, M. K., Kim, H., Kim, K., Song, W. J., and Chung, S. H. (2010) *J. Neurochem.* **115,** 574–584
15. Smith, D. J., Stevens, M. E., Sudanagunta, S. P., Bronson, R. T., Makhinson, M., Watabe, A. M., O'Dell, T. J., Fung, J., Weier, H. U., Cheng, J. F., and Rubin, E. M. (1997) *Nat. Genet.* **16,** 28–36
16. Ahn, K. J., Jeong, H. K., Choi, H. S., Ryoo, S. R., Kim, Y. J., Goo, J. S., Choi, S. Y., Han, J. S., Ha, I., and Song, W. J. (2006) *Neurobiol. Dis.* **22,** 463–472
17. Altafaj, X., Dierssen, M., Baamonde, C., Martí, E., Visa, J., Guimerà, J., Oset, M., González, J. R., Flórez, J., Fillat, C., and Estivill, X. (2001) *Hum. Mol. Genet.* **10,** 1915–1923
18. Tejedor, F. J., and Hammerle, B. (2011) *FEBS J.,* **278,** 223–235
19. Davies, K. J., Ermak, G., Rothermel, B. A., Pritchard, M., Heitman, J., Ahnn, J., Henrique-Silva, F., Crawford, D., Canaider, S., Strippoli, P., Carinci, P., Min, K. T., Fox, D. S., Cunningham, K. W., Bassel-Duby, R., Olson, E. N., Zhang, Z., Williams, R. S., Gerber, H. P., Pérez-Riba, M., Seo, H., Cao, X., Klee, C. B., Redondo, J. M., Maltais, L. J., Bruford, E. A., Povey, S., Molkentin, J. D., McKeon, F. D., Duh, E. J., Crabtree, G. R., Cyert, M. S., de la Luna, S., and Estivill, X. (2007) *FASEB J.* **21,** 3023–3028
20. Porta, S., Martí, E., de la Luna, S., and Arbonés, M. L. (2007) *Eur. J. Neurosci.* **26,** 1213–1226
21. Hoeffer, C. A., Dey, A., Sachan, N., Wong, H., Patterson, R. J., Shelton, J. M., Richardson, J. A., Klann, E., and Rothermel, B. A. (2007) *J. Neurosci.* **27,** 13161–13172
22. Chang, K. T., Shi, Y. J., and Min, K. T. (2003) *Proc. Natl. Acad. Sci. U.S.A.* **100,** 15794–15799
23. Porta, S., Serra, S. A., Huch, M., Valverde, M. A., Llorens, F., Estivill, X., Arbonés, M. L., and Martí, E. (2007) *Hum. Mol. Genet.* **16,** 1039–1050
24. Keating, D. J., Dubach, D., Zanin, M. P., Yu, Y., Martin, K., Zhao, Y. F., Chen, C., Porta, S., Arbonés, M. L., Mittaz, L., and Pritchard, M. A. (2008) *Hum. Mol. Genet.* **17,** 1020–1030
25. Arron, J. R., Winslow, M. M., Polleri, A., Chang, C. P., Wu, H., Gao, X., Neilson, J. R., Chen, L., Heit, J. J., Kim, S. K., Yamasaki, N., Miyakawa, T., Francke, U., Graef, I. A., and Crabtree, G. R. (2006) *Nature* **441,** 595–600
26. Harris, C. D., Ermak, G., and Davies, K. J. (2007) *FEBS J.* **274,** 1715–1724
27. Ferrer, I., Barrachina, M., Puig, B., Martínez de Lagrán, M., Martí, E., Avila, J., and Dierssen, M. (2005) *Neurobiol. Dis.* **20,** 392–400
28. Ermak, G., Morgan, T. E., and Davies, K. J. (2001) *J. Biol. Chem.* **276,** 38787–38794
29. Fuentes, J. J., Genescà, L., Kingsbury, T. J., Cunningham, K. W., Pérez-Riba, M., Estivill, X., and de la Luna, S. (2000) *Hum. Mol. Genet.* **9,** 1681–1690
30. Kaech, S., and Banker, G. (2006) *Nat. Protoc.* **1,** 2406–2415
31. Zeitelhofer, M., Vessey, J. P., Xie, Y., Tübing, F., Thomas, S., Kiebler, M., and Dahm, R. (2007) *Nat. Protoc.* **2,** 1692–1704
32. Sagoo, J. K., Fruman, D. A., Wesselborg, S., Walsh, C. T., and Bierer, B. E. (1996) *Biochem. J.* **320**, 879–884
33. Vega, R. B., Yang, J., Rothermel, B. A., Bassel-Duby, R., and Williams, R. S. (2002) *J. Biol. Chem.* **277,** 30401–30407
34. Nishi, Y., and Lin, R. (2005) *Dev. Biol.* **288,** 139–149
35. Poppek, D., Keck, S., Ermak, G., Jung, T., Stolzing, A., Ullrich, O., Davies, K. J., and Grune, T. (2006) *Biochem. J.* **400,** 511–520
36. Martínez-Martínez, S., Genescà, L., Rodríguez, A., Raya, A., Salichs, E., Were, F., López-Maderuelo, M. D., Redondo, J. M., and de la Luna, S. (2009) *Proc. Natl. Acad. Sci. U.S.A.* **106,** 6117–6122
37. Chan, B., Greenan, G., McKeon, F., and Ellenberger, T. (2005) *Proc. Natl. Acad. Sci. U.S.A.* **102,** 13075–13080
38. Lee, E. J., Seo, S. R., Um, J. W., Park, J., Oh, Y., and Chung, K. C. (2008) *J. Biol. Chem.* **283,** 3392–3400
39. Wegiel, J., Gong, C. X., and Hwang, Y. W. (2011) *FEBS J.* **278,** 236–245
40. Wegiel, J., Kaczmarski, W., Barua, M., Kuchna, I., Nowicki, K., Wang, K. C., Wegiel, J., Yang, S. M., Frackowiak, J., Mazur-Kolecka, B., Silverman,

W. P., Reisberg, B., Monteiro, I., de Leon, M., Wisniewski, T., Dalton, A., Lai, F., Hwang, Y. W., Adayev, T., Liu, F., Iqbal, K., Iqbal, I. G., and Gong, C. X. (2011) *J. Neuropathol. Exp. Neurol.* **70,** 36–50
41. Pfister, S. C., Machado-Santelli, G. M., Han, S. W., and Henrique-Silva, F. (2002) *BMC Cell Biol.* **3,** 24
42. de la Luna, S., and Estivill, X. (2006) *Trends Mol. Med.* **12,** 451–454
43. Liu, Q., Busby, J. C., and Molkentin, J. D. (2009) *Nat. Cell Biol.* **11,** 154–161
44. Abbasi, S., Lee, J. D., Su, B., Chen, X., Alcon, J. L., Yang, J., Kellems, R. E., and Xia, Y. (2006) *J. Biol. Chem.* **281,** 7717–7726
45. Hilioti, Z., Gallagher, D. A., Low-Nam, S. T., Ramaswamy, P., Gajer, P., Kingsbury, T. J., Birchwood, C. J., Levchenko, A., and Cunningham, K. W. (2004) *Genes Dev.* **18,** 35–47
46. Rothermel, B., Vega, R. B., Yang, J., Wu, H., Bassel-Duby, R., and Williams, R. S. (2000) *J. Biol. Chem.* **275,** 8719–8725
47. Genescà, L., Aubareda, A., Fuentes, J. J., Estivill, X., De La Luna, S., and Pérez-Riba, M. (2003) *Biochem. J.* **374,** 567–575
48. Mehta, S., Li, H., Hogan, P. G., and Cunningham, K. W. (2009) *Mol. Cell. Biol.* **29,** 2777–2793
49. Mulero, M. C., Aubareda, A., Orzáez, M., Messeguer, J., Serrano-Candelas, E., Martínez-Hoyer, S., Messeguer, A., Pérez-Payá, E., and Pérez-Riba, M. (2009) *J. Biol. Chem.* **284,** 9394–9401
50. Aubareda, A., Mulero, M. C., and Pérez-Riba, M. (2006) *Cell. Signal.* **18,** 1430–1438
51. Garver, T. D., Kincaid, R. L., Conn, R. A., and Billingsley, M. L. (1999) *Mol. Pharmacol.* **55,** 632–641
52. Abdul, H. M., Sama, M. A., Furman, J. L., Mathis, D. M., Beckett, T. L., Weidner, A. M., Patel, E. S., Baig, I., Murphy, M. P., LeVine, H., 3rd, Kraner, S. D., and Norris, C. M. (2009) *J. Neurosci.* **29,** 12957–12969
53. Abdul, H. M., Furman, J. L., Sama, M. A., Mathis, D. M., and Norris, C. M. (2010) *Mol. Cell Pharmacol.* **2,** 7–14
54. Cook, C. N., Hejna, M. J., Magnuson, D. J., and Lee, J. M. (2005) *J. Alzheimers Dis.* **8,** 63–73
55. Yang, J., Rothermel, B., Vega, R. B., Frey, N., McKinsey, T. A., Olson, E. N., Bassel-Duby, R., and Williams, R. S. (2000) *Circ. Res.* **87,** E61–E68